ENHANCED RADIOMETRIC FUNCTIONS FOR HOMOGENEOUS MATERIALS

Dr. Khalil I. Jassam, Department of Surveying Engineering
University of Maine Orono, ME 04473, USA
Commission No:II

Abstract:
This paper discusses the development , analysis, and mathematical modeling of radiometric functions for homogeneous materials. These functions express changes in the intensity of reflected light with variations in surface orientation and location of light source. Four samples of materials with constant spectral reflectance --white sand, brown sand, styrofoam and barium sulfate-- were used to develop the radiometric functions. The samples were studied at the blue,green, red, and infrared energy bands. Data collection procedures took place in both laboratory and outdoor environments. The four samples reflected light in a similar manner in all wavelengths in lab and outdoor environments. A simple sine and cosine function with different coefficients fitted the collected data. The technique can potentially be used in mapping desert and snow covered areas from a single satellite image. Accuracy of maps generated will be tested and presented in a later paper.

Key Words: Radiometric, Photometric Function, Mapping from a Single Photo.

INTRODUCTION

In the 1960's scientists were trying to map part of the lunar surface in conjunction with man landing on it. At that point no stereo coverage was available, meaning conventional mapping techniques could not be used. One of the possible solutions was development of a mathematical model to relate lunar brightness to terrain elevation.
Work at the Jet Propulsion Laboratory (JPL, 1963) showed that the brightness (B) of any element on the lunar surface can be expressed in terms of three angles;

$$B\ (i,e,g) = \rho\ E_O f(i,e,g) \quad \text{.....(1)}$$

where:
B is the brightness of any element,
ρ is the surface reflectance coefficient,
E_O is the uniform illumination intensity,
i is the incidence angle for surface radiometric geometry (the angle between the incident ray and the surface normal),
e is the emission angle for surface radiometric geometry (the angle between the reflected ray and the surface normal), and
g is the phase angle for the surface radiometric geometry (the angle between the incident ray and the reflected or emitted ray).
figure 1 shows the three angles.

Researchers at JPL recognized a problem even if they could describe the lunar brightness in terms of the three radiometric angles (i, e, g). The model (function) could not be used for mapping purposes because of too many unknown parameters. To illustrate the point, equation 1 can be rewritten when E_O and ρ are considered constant (single photo of homogeneous materials) :

$$B = f(i,\ e,\ g) \quad \text{.....(2)}$$

B for any point on an object can be measured with a radiometer. The phase angle (g) can be computed if the sensor and light positions are available. This will leave two unknowns, i and e, which are both dependent on the direction of the normal to the surface. It became clear that a radiometric function defined in terms of three angles is useless for mapping purposes because of too many unknowns. Researchers were required to seek an alternative approach to solve the problem.

RADIOMETRIC FUNCTION IN TERMS OF TWO ANGLES

Rinfleisch (1966) proved that the radiometric function for the lunar surface can be approximated in terms of two angles. These angles are the phase angle (g) and the auxiliary angle (α). The auxiliary angle is between the normal to the surface and the projection of the sensor onto the plane defined by the incident and reflected rays (figure 2). Equation 1 can be rewritten:

$$B\ (i,\ e,\ g) = \rho\ E_O f(g,\alpha) \quad \text{.....(3)}$$

Brightness (B) can be measured and phase angle (g) can be mathematically computed. Therefore, the only unknown in equation 3 is the auxiliary angle (α). The auxiliary angle (α) is a function of the normal to the surface, it directly relate to the terrain shape. This technique was used to map part of the lunar surface at full moon (sun behind observer) in the mid-1960's, (Rinfleisch, 1966)

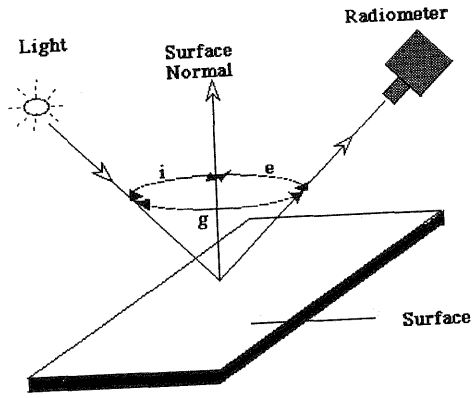

Figure 1. The Three Radiometric Angles

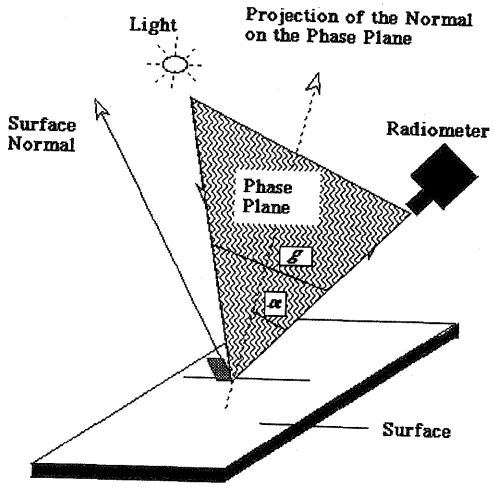

Figure 2. The Two Radiometric Angles

RADIOMETRIC FUNCTIONS FOR PART OF EARTH'S SURFACE

Subsequent to the lunar exploration program one finds no published attempts to modify the discussed technique to map the earth's surface. However, Horn (1975) attempted to use the same idea for industrial applications. He concluded that "the moon is a unique case," and that an objects shape cannot be obtained without further assumptions if only one photo is used. Up to date literature search shows no published papers in this area, therefore it can be concluded that reflected light radiometric functions have not been develop for the earth's homogeneous surfaces (sand dunes, snow coverage, etc).

A special instrument was constructed at the University of Wisconsin - Madison to collect the data necessary for the understanding and developing of a mathematical functions between light intensity and the two radiometric angles (g and α). The instrument consisted of a wooden structure designed to carry the sensor and light source in a way that each could easily be independently moved. The instrument was also designed to guarantee the coplanar motion of the sensor and light source. This arrangement facilitated measurement of both g and α angles. (figures 3 and 4)

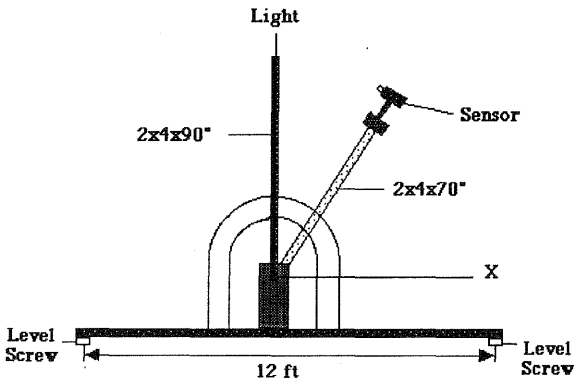

Figure 3. Instrument Front View

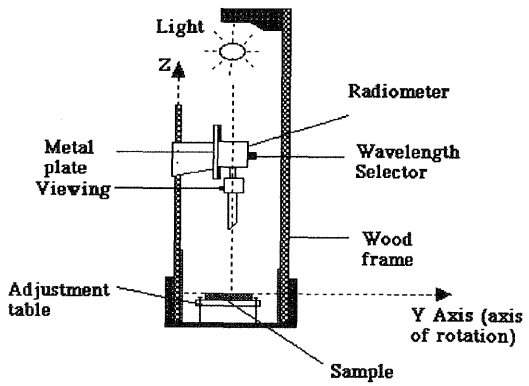

Figure 4. Side View of The instrument

DATA ACQUISITION

In order to model the radiometric functions, four homogenous materials where investigated. These materials included white sand, brown sand, styrofoam, and barium sulfate. Each material was studied under laboratory and out door environments. Blue (0.450 μm), green (0.550 μm), red (0.650 μm), and infrared (0.900 μm) wavelengths were tested.

In the lab environment data was collected in a dark room with one source of light. The dark room minimized the effect of diffuse light, eliminated complicated shadow arising from multiple light sources, thus created an environment similar to that of the lunar surface. The sign of both the phase and the auxiliary angles were considered positive if the light source is above the sensor and negative if the light was below the sensor. The phase angle ranged from -60 to 140 degrees, the auxiliary angle from -70 to 70 degrees.

All combinations of 10 degrees increment were tested for both angles (figure 5). The procedure was repeated for all samples.

Out door data was collected in a similar procedure, but the instrument had to be modified to ensure that the sensor, sun and the normal to the sample were in the same plane (figure 6). It should be pointed out that in this case, the phase angle ranged from -40 to 150 degrees and the auxiliary angle from -70 to 70 degrees.

The standard deviation (σ) of unit measurement for all samples at both the lab and out door was computed, by repeating the same measurement 10 times. The value of (σ) depends on the sample spectral properties and wavelength sensitivity to light.

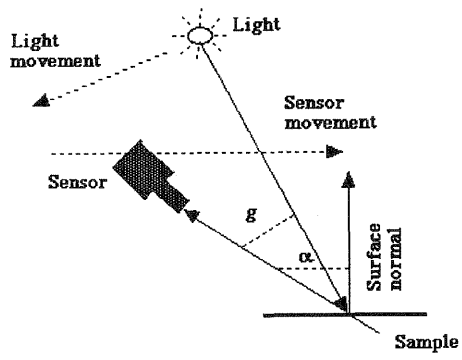

Figure 5. Lab Data Collection

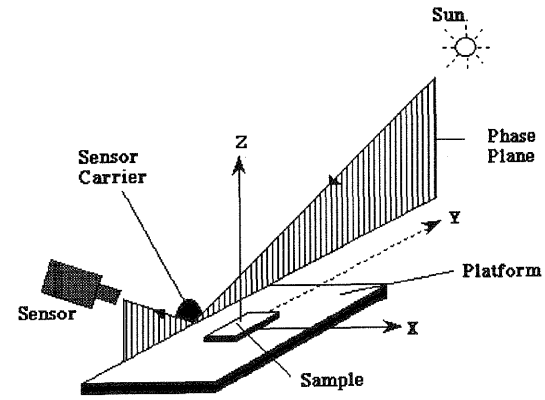

Figure 6. Out Door Data Collection

DATA REDUCTION AND ANALYSIS

A tabular listing of the data allowed comparison of reflected light intensity for any combinations. It also illustrated the consistency of the data so that development of the radiometric function appeared possible. The colleted data took the form of a banded matrix. Cross sections were taken to understand the behavior of light intensity with the phase and the auxiliary angles individually (figure 7). The cross sections were obtained for all samples, wavelengths, and for lab and out door environments (figure 8, 9, 10 and 11).They provided a powerful tool to compare different wavelengths and samples behavior. They clearly showed that light intensity increased with the auxiliary angle and decreased with the phase angle for both lab and out door. In the lab environment, green wavelength light was the most sensitive to the light intensity and IR the least, with the exception of brown sand where red was the most sensitive. In the out door, blue light was the most sensitive and the IR the least. This is an expected result due to the scattering of blue light in a sunny day. The differences between samples were obvious, in both cases the styrofoam was the most sensitive, and white sand the least in the lab and brown sand the least out door. This might be related to the spectral properties of brown sand.

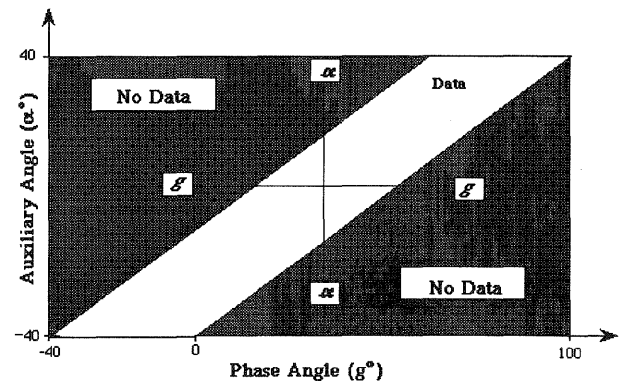

Figure 7. Data Shape and Cross Sections in the Direction of Both g and α

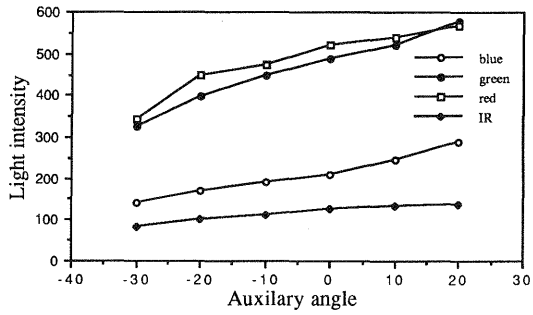

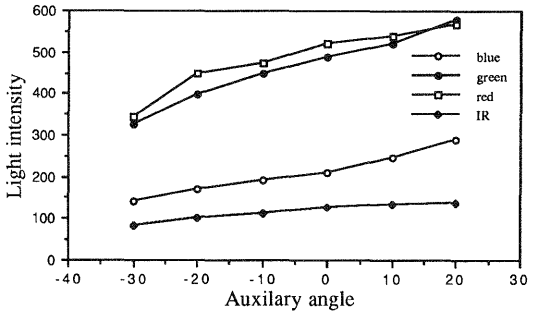

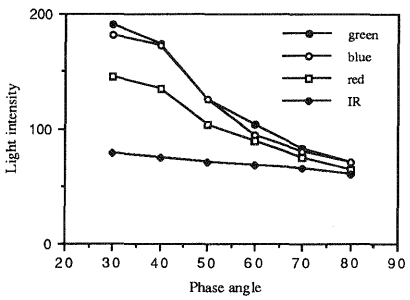

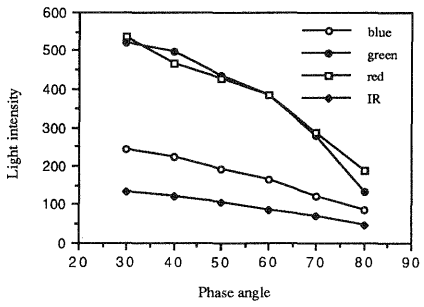

Figure 8. Variation of light intensity with the phase (g) and auxiliary angles (a) for Brown sand at both the lab and out door, (a) lab data, (b) field data, (c) lab data, and (d) is field data.

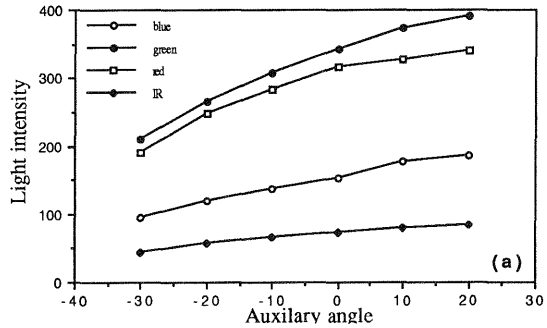

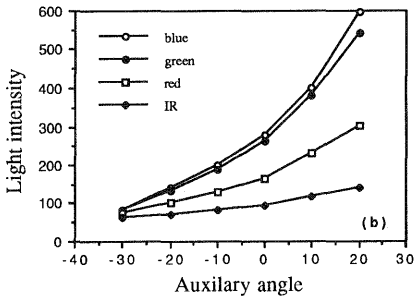

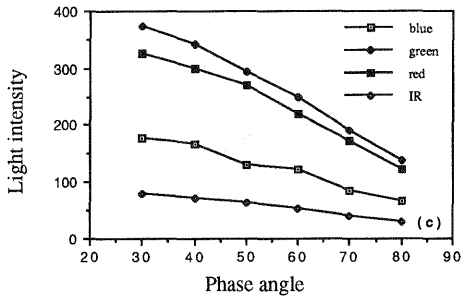

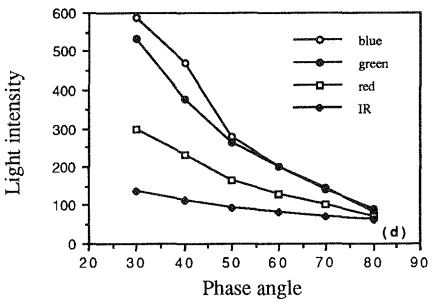

Figure 9. Variation of light intensity with the phase (g) and auxiliary angle (α) for White sand at both the lab and out door, (a) lab data, (b) field data, (c) lab data, and (d) field data.

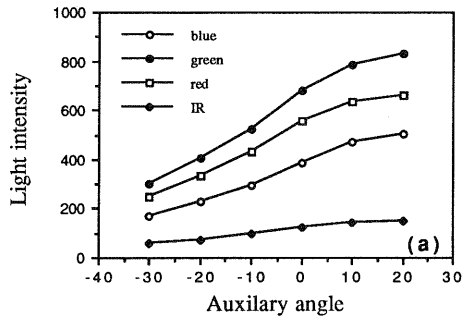

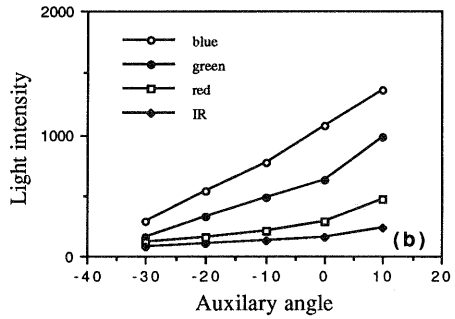

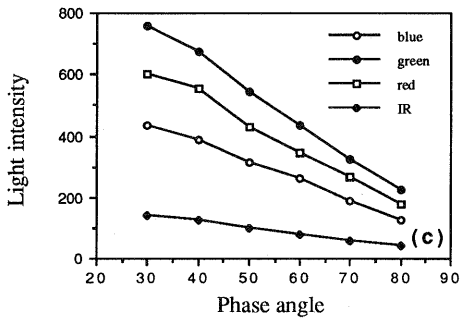

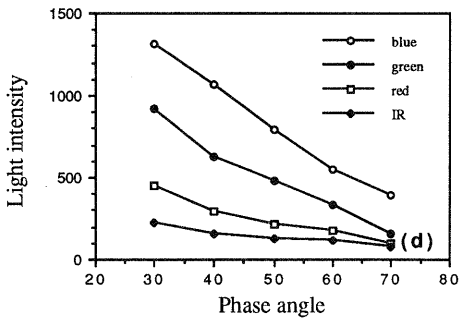

Figure 11. Varation of light intesnsity with the phase (g) and auxiliary (a) angles for styrofoam at both lab and out door, (a) lab data, (b) field data, (c) lab data, and (d) field data.

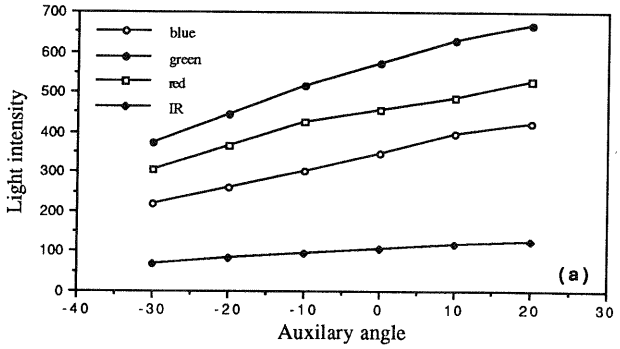

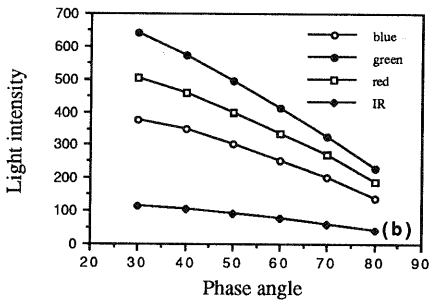

Figure 10. Variation of light intensity with the phase (g) and auxiliary angle (a) for Barium sulfate lab data.

MATHEMATICAL MODELING

Data analysis showed that all samples acted in a similar fashion in both lab and out door environments. This suggested that the radiometric function for all samples might be fitted by one model with different coefficients. Theoretically, there are an infinite number of mathematical models. However, one would expect that the function might be similar to the lunar radiometric function, due to similarity of environment and the homogeneity of the samples.The lunar radiometric function was a combination of sine and cosine of the two radiometric angle g and α.

The models tested included:

$$B = a_0 + a_1 \sin g + a_2 \sin \alpha + a_3 \cos g + a_4 \cos\alpha + a_5 {}^2\sin g + a_6 \sin^2\alpha + a_7 \cos^2 g + a_8 \cos^2\alpha + a_9 \sin^3 g + a_{10} \sin^3 \alpha \quad \text{.....(4)}$$

$$B = a_0 + a_1 \cos g + a_2 \sin \alpha + a_3 \cos \alpha + a_4 \sin g + a_5 \cos g \sin \alpha + a_6 \sin g \cos \alpha + a_7 \cos g \cos \alpha + a_8 \sin g \sin \alpha \quad \text{.....(5)}$$

$$B = a_0 + a_1 \cos g + a_2 \sin \alpha + a_3 \cos \alpha + a_4 \sin g + a_5 \cos 2g + a_6 \sin 2\alpha + a_7 \cos 2\alpha + a_8 \sin 2g + a_9 \cos 3g + a_{10} \cos 3 \alpha \quad \text{.....(6)}$$

where :
B, g, and α were previously defined, and $a_0 \ldots a_{10}$ are coefficients of the function.

The three models were tested by least square adjustment and the model in equation 6 seems to fit the data the best, for all samples and wavelengths in both lab and out door environments. Further tests proved that only four coefficients are needed to obtain statically the same coefficients based on resulting values of standard deviation.

The radiometric function for all tested materials in both lab and out door environments is

$$B= a_0 + a_1 \cos g + a_2 \sin 2g + a_3 \sin \alpha \quad \text{.....(8)}$$

It should be pointed that the coefficients are different for each sample and wavelength.

CONCLUSIONS, AND FUTURE RESEARCH

The radiometric function for four homogenous materials at different wavelengths was developed. All samples acted in similar pattern at both lab and out door environments. The radiometric function can be potentially contribute to mapping technology by providing an inexpensive alternative for mapping desert and snow covered area using aerial or satellite images. It also can be used for mapping dynamic objects such ocean surface. Future research toward utilizing this technique for the above and other applications should be continue. This same idea might be applicable for mapping form a single radar image. since it proved that the surface orientation and local incident angle contribute to the strength of the SAR signal.

REFERENCES

1. Herriman, A.G., Washburn, H.W. and D.E. Willingham, 1963, "Ranger Preflight Science Analysis and the Lunar photometric Model," Jet Propulsion Laboratory Technical Report No. 32-384.

2. Horn, B.K.P., 1975, "Obtaining Shape from Shading Information, The Psychology of Computer Vision, McGraw-Hill, USA, pp. 115-155.

3. Jassemm, K.I., 1985, "photometric Functions for Mapping from a Single Photograph," Ph. D. dissertation, University of Wisconsin, Madison.

4. Rindfleisch, T., 1966, "photometric Method for Lunar Topography," Photgrammetric Engineering, Vol. 32, pp. 262-276.

5. Waston, K., 1968, Photoclinometry from Space Craft Images: U.S. Geological Survey Prof. Paper 599-B, 10 p.